International Immunopharmacology 66 (2019) 109–118

Contents lists available at ScienceDirect

International Immunopharmacology

journal homepage: www.elsevier.com/locate/intimp

The novel *N*-methyl-D-aspartate receptor antagonist MN-08 ameliorates lipopolysaccharide-induced acute lung injury in mice

Jinxin Jiang, Qianqian Jian, Mei Jing, Zaijun Zhang, Gaoxiao Zhang, Luchen Shan, Pei Yu, Yuqiang Wang, Lipeng Xu*

Jinan University, College of Pharmacy, Guangzhou 510632, China

ARTICLE INFO

Keywords:
MN-08
NMDAR
Inflammation
Oxidative stress
Tight junctions
Acute lung injury

ABSTRACT

Acute lung injury (ALI) is a clinically severe respiratory disorder, and effective therapy is urgently needed. MN-08, a novel synthetic *N*-methyl-D-aspartate receptor (NMDAR) antagonist, was investigated for its effect on lipopolysaccharide (LPS)-induced ALI. In vitro, the protective effect of MN-08 on inflammatory response, oxidative stress, and tight junctions (TJs) structure was explored in LPS-induced RAW 264.7 cells and A549 cells. MN-08 markedly decreased ($p < 0.001$) the levels of pro-inflammatory cytokines such as tumor necrosis factor-α (TNF-α), interleukin-1β (IL-1β), cyclooxygenase-2 (COX-2), inducible nitric oxide synthase (iNOS), and reactive oxygen species (ROS), whereas it moderately upregulated ($p < 0.05$) heme oxygenase (HO)-1 protein expression in LPS-induced RAW 264.7 cells. Moreover, MN-08 significantly inhibited ($p < 0.001$) cell apoptosis and improved ($p < 0.001$) protein expression of TJs in LPS-induced A549 cells. In vivo, the therapeutic effect of MN-08 was evaluated in the LPS-induced ALI model through intratracheal instillation in BALB/c mice. MN-08 administration dramatically attenuated ($p < 0.001$) pulmonary pathological changes and reduced ($p < 0.001$) the levels of glutamate, myeloperoxidase (MPO), malondialdehyde (MDA), and number of cells in BALF, whereas it increased ($p < 0.05$) superoxide dismutase (SOD) and glutathione (GSH) activities in ALI mice. Furthermore, MN-08 markedly blocked the mitogen-activated protein kinases (MAPKs)/nuclear translocation of nuclear factor-κB (NF-κB) signaling pathways in RAW 264.7 cells and lung tissues. These results indicate that MN-08 exhibits lung protection in an LPS-induced ALI model via anti-inflammatory and anti-oxidative activities.

1. Introduction

Acute lung injury (ALI) and acute respiratory distress syndrome (ARDS) are severe respiratory disorders that cause significantly high morbidity and mortality (~30%–50%) [1]. The physiologic characteristics of ALI are disruption in the microvascular endothelial barrier, pulmonary edema, uncontrolled inflammation, and intrapulmonary hemorrhage [2]. Many conditions, such as sepsis, pneumonia, inhalation injury, pancreatitis, and burns can lead to ALI [3,4]. Despite the great efforts and contributions of the experts, there is still an urgent need to develop new therapies to treat patients with ALI.

As a pathogenic component of endotoxin in the outer membrane of gram-negative bacteria, lipopolysaccharide (LPS) could induce an inflammatory response and lead to the disturbance of the immune system function, which is extensively used to induce ALI of BALB/c mice by intratracheal instillation [5–7]. As is widely accepted, LPS is an important trigger of the lung inflammation that is regulated by nuclear factor-kappa B (NF-κB) and mitogen-activated protein kinases (MAPKs), including the c-Jun NH2-terminal kinase (JNK), extracellular signal-regulated kinase (ERK), and the p38 MAPKs pathways [8,9]. Accumulating evidences suggest that NF-κB and MAPKs play critical roles in the overexpression of inflammatory mediators such as tumor necrosis factor-α (TNF-α), interleukin-1β (IL-1β), and interleukin-6 (IL-6) [10,11]. Inflammatory mediators also activate alveolar epithelial cells, pulmonary vascular endothelial cells, and chemotactic neutrophils, which could lead to cell dysfunction, alveolar capillary endothelial damage, and increased pulmonary permeability. Moreover, under oxidative stress conditions, nuclear factor erythroid 2-related factor 2 (Nrf2) dissociates from Kelch-like ECH-associated protein 1 (Keap1), translocates into the nucleus, and binds to the antioxidant response element (ARE) to initiate transcription of Nrf2 downstream target genes. As an internal target gene of the anti-oxidant system Nrf2 downstream, the expression of catalase (CAT), superoxide dismutase (SOD), glutathione (GSH), and heme oxygenase (HO-1) could help maintain the homeostasis of redox status [12,13].

Tight junctions (TJs) are the structure and foundation of pulmonary

* Corresponding author.
E-mail address: xulipeng2000@163.com (L. Xu).

https://doi.org/10.1016/j.intimp.2018.11.010
Received 1 July 2018; Received in revised form 7 November 2018; Accepted 8 November 2018
Available online 14 November 2018

capillaries. TJ proteins are composed of transmembrane proteins, cytosolic attachment proteins, and cytoskeletal proteins, which are important factors to maintain the integrity of lung tissue permeability. For instance, occludin is the main structural protein of TJs and is necessary to maintain low pulmonary capillary osmotic pressure. Claudins are major components of the TJ complex, and they maintain TJ selection permeability and cellular polarization. JAM-1 is a kind of molecule in transmembrane protein that mediates the binding between cells or between cells and matrix. ZO-1 is associated with maintaining and regulating epithelial and barrier function [14–17]. Decades of research have shown that TJ changes play vital roles in the disruption of the pulmonary epithelial barrier during ALI. Maintenance of barrier properties requires the integrity of epithelial TJs. Disruption of the endothelial and epithelial barrier may lead to altered pulmonary permeability [18,19]. Our study aimed to discover whether MN-08 could exhibit a protective effect on anti-inflammatory response and anti-oxidative damage in the process of cell apoptosis and TJ changes.

Glutamate, an important neurotransmitter that mediates most synaptic excitations, has the highest content in the central nervous system (CNS) and is involved in many important physiological functions in the brain. Excitatory toxicity is caused by a variety of factors, such as massive release of glutamate and accumulation in the synaptic cleft, which leads to excessive activation of glutamate receptor and causes a series of pathological and physiological changes ending with the death of nerve cells [20]. *N*-methyl-D-aspartate receptors (NMDARs) have recently been studied in peripheral neural structures, including the respiratory system, the renal system, pancreatic islets, and blood vessels [21–24]. Similar to neurons, mononuclear leukocytes and neutrophils can release glutamate in non-neuronal cells and tissues [25]. Under pathological conditions, extracellular glutamate concentration is increased abnormally, which could overactivate glutamate receptors and finally leads to inflammatory cytokine production and ROS formation [26]. In a previous study, we designed and synthesized a novel memantine derivative MN-08 (with a purity > 98%; Fig. 1A) that acts as a NMDAR antagonist. Moreover, we determined the LD_{50} value of MN-08 in mice. The LD_{50} values of MN-08 and memantine are 58 mg/kg and 46 mg/kg, in a single intravenous dose. Since the MWs of MN-08 and memantine are 290 and 215, respectively, the LD_{50} value of MN-08 and memantine are basically the same on a molar basis. Moreover, MN-08 has a good PK profile and its tissue distribution to the lungs is approximately 29% [27]. Although the effect of MN-08 could contribute to cortical neurons [28], the protective effects in lung injury and the mechanisms of action had not been clarified to date. Our research provides scientific and rigorous evidence that MN-08 might exert lung protection by anti-inflammatory and anti-oxidative activities.

2. Materials and methods

2.1. Materials

MN-08 and memantine (Mem) were synthesized in our laboratory with a purity of > 98%. LPS (*Escherichia coli* 0111:B4), dexamethasone (Dex), methyl thiazolyl tetrazolium (MTT), dimethyl sulfoxide (DMSO), and 2′,7′-dichlorofluorescein-diacetate ($DCFH_2$-DA) were purchased from Sigma-Aldrich (St. Louis, MO, USA). Antibodies against NF-κB p65, p-NF-κB p65, IκBα, p-IκBα, p-(ERK1/2), ERK1/2, p-(JNK1/2), JNK1/2, p-(p38 MAPK), p38 MAPK, HO-1, glyceraldehyde-3-phosphate dehydrogenase (GAPDH), β-actin, and horseradish peroxidase (HRP)-conjugated goat anti-rabbit were purchased from Cell Signaling (Boston, MA, USA). Antibodies against anti-Zonula occludens 1 (ZO-1), occludin, anti-junctional adhesion molecule 1 (JAM-1), Claudin-1, Gr-1, Mac-2 and CD163 were purchased from Abcam (Cambridge, MA). IL-1β and TNF-α enzyme-linked immunosorbent assay (ELISA) kits, MPO, SOD, MDA, GSH, and glutamate detection kits were purchased from Nanjing Jiancheng Bioengineering Institute (Nanjing, China). Isoflurane was purchased from Rick ward (RWD LIFE SCIENCE).

2.2. Animals and study design

All studies were performed in accordance with the standards set forth in the eighth edition of Guide for the Care and Use of Laboratory animals, which was published by the National Academy of Sciences, The National Academies Press, Washington D.C. Animal studies performed here adhere to ethical guidelines of The Basel Declaration, and were approved by the ethics committee of the Jinan University. Male BALB/c mice, 6 to 8 weeks of age and weighing 18 to 20 g, were obtained from the Sun Yat-sen University Laboratory Animal Center (Certificate SYXK 2011-0112, Guangzhou, Guangdong, China). All animals were housed in a room at a temperature of 24 °C ± 1 °C under a 12-hour light/dark cycle with a relative humidity of 40% to 80%. The mice were given adequate food and water for several days to adapt to the environment before experimentation.

Male BALB/c mice (n = 56) were randomly divided into seven groups, as follows: Group 1: Sham (n = 8); Group 2: LPS (n = 8); Group 3: LPS + MN-08 (6.25 mg/kg, n = 8); Group 4: LPS + MN-08 (12.5 mg/kg, n = 8); Group 5: LPS + MN-08 (25 mg/kg, n = 8); Group 6: LPS + Dex (5 mg/kg, n = 8) and Group 7: LPS + Mem (10 mg/kg, n = 8). As the core skeleton of MN-08, Mem is used for structure-effect comparison. Dex, a classic anti-inflammatory drug, is often used as a positive control drug [29–31]. MN-08, Dex, or Mem was dissolved in normal saline (NS) and administered via tail vein injection. The sham group and the LPS group were administered NS via tail vein injection.

The mice were anesthetized with isoflurane, and LPS was administered by intratracheal instillation with 50 μL LPS (1 mg/kg) to induce the ALI model. Then, mice were treated with drugs at 1 h and 6 h. After 12 h of LPS administration, the animals were euthanized with 4% (w/v) chloral hydrate solution. Accordingly, plasma, bronchoalveolar lavage fluid (BALF), and lung tissue samples were harvested for further experiments.

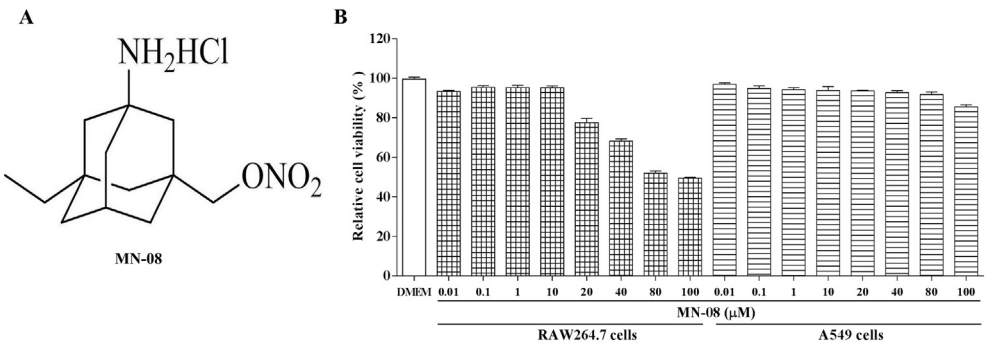

Fig. 1. The structure of MN-08 and cytotoxicity of MN-08 in RAW 264.7 cells and A549 cells.

2.3. Cells culture and viability assay

The RAW 264.7 macrophages are used in a model of LPS-induced ALI, and macrophages play an essential role in the regulation of inflammation responses [32,33]. The human type II lung epithelial A549 cell line plays a critical role in the pathogenesis of LPS-induced ALI [34,35]. Increasing studies demonstrate that A549 cell lineages are usually used to build cell apoptosis models in LPS-induced ALI. The RAW 264.7 macrophage and A549 cell lines were obtained from the American Type Culture Collection (ATCC, Rockville, MD). Cells were cultured in Dulbecco modified Eagle medium (DMEM) or Roswell Park Memorial Institute (RPMI)-1640 containing 10% (v/v) fetal bovine serum and 1% (v/v) penicillin/streptomycin at 37 °C in a humidified incubator with 5% CO_2. Cell viability was determined by MTT assay. RAW 264.7 or A549 cells were cultured in a 96-well plate for 24 h. Cells were then treated with various concentrations of MN-08 for another 24 h. MTT was added to incubate for 4 h at 37 °C. The formazan crystal was dissolved with DMSO, and the absorbance was measured at 490 nm using a microplate reader (Bio-Tek Instruments Inc.).

2.4. Intracellular ROS measurement

To measure ROS generation, RAW 264.7 cells were cultured in 96-well plates (1×10^4 cells/well) for 24 h. Cells were pretreated with MN-08 and Dex for 1 h, then LPS was added to the plates for an additional 24 h. Next, the cells were stained with 100 μL of dichlorofluorescein diacetate ($DCFH_2$-DA) (10 μM) for 30 min and washed with Hank's balanced salt solution (HBSS) three times. The intracellular levels of ROS were analyzed by a multi-detection reader (Bio-Tek Instruments Inc.) at excitation wavelengths of 488 nm and emission wavelengths of 525 nm, respectively.

2.5. Lung wet/dry weight ratio

Lung tissues were rinsed with phosphate-buffered saline (PBS), dried with absorbing paper, and immediately weighed to obtain the wet weight (W); then, tissues were placed in an oven at 60 °C for 48 h to assess the dry weight (D). The W/D ratio was calculated to evaluate the lung edema.

2.6. Cell count and total protein in BALF

In the left lung tissue, the cannula was inserted through the cervical trachea, and the trachea and trocar were fixed and sealed with a silk thread through the tracheal esophageal space. The left lung was distended with 0.5 mL autoclaved and pre-cooling PBS buffer, and the fluid was recovered three times up to a total volume of 1.5 mL. The BALF was centrifuged (4 °C, 1500 rpm) for 10 min, and the supernatant was shifted to new tubes and stored at −80 °C. The sediment cells were resuspended with PBS buffer. The total cells in BALF were counted with a hemocytometer under optical microscopy, and cytospins were prepared for leukocyte differential counting by staining with Wright-Giemsa stain. Total protein in the supernatant of the BALF was quantified using a bicinchoninic acid (BCA) protein assay kit to evaluate vascular permeability in the alveolar capillaries.

2.7. Enzyme-linked immunosorbent assay (ELISA)

Levels of pro-inflammatory cytokines TNF-α and IL-1β in cell supernatants or plasma were quantified with ELISA kits according to the manufacturer's instructions.

2.8. Lung tissues for biochemical analysis

The lung tissues were homogenized and dissolved in extraction buffer to analyze glutamate, MPO, MDA, SOD, and GSH levels by using commercially available assay kits in accordance with the manufacturer's protocols.

2.9. Pathological evaluation of lung injury

One lobe of tissue from the right lung was fixed with 4% (w/v) paraformaldehyde. Samples were dehydrated in a series of graded ethanol, embedded in paraffin, and cut into 5-μm-thick sections. The paraffin-embedded sections were stained with hematoxylin-eosin (H&E) and analyzed under light microscopy. In each section, five random areas were examined at ×100 magnification and ×400 magnification, and random blind statistics were used.

2.10. Immunohistochemistry examination

Lung sections were hydrated and epitope retrieval was performed according to the manufacturer's protocol (GTVision™ III detection system Mo&Rb, Shanghai, China). Then, the sections were stained with primary antibodies against Gr-1, Mac-2, ZO-1 and JAM-1 followed by secondary HRP-labeled polymer with DAB staining. In each section, five random areas were examined at ×100 magnification, and random blind statistics were used.

2.11. Immunofluorescence observation

Lung tissues were embedded in paraffin and cut into 5-μm-thick sections. The sections were subjected to xylene and gradient ethanol dewaxing hydration, antigen repaired, followed by PBS rinsing. Then, sections were sealed with 10% goat serum for 30 min and stained with primary antibodies against TNF-α (1:200) and HO-1 (1:400) and CD163 (1:250) at 4 °C overnight. After rinsing with PBS, the sections were incubated for 30 min with Alexa Fluor® 488-conjugated Affinipure Donkey anti-mouse IgG (H + L) and Alexa Fluor® 647-conjugated Affinipure goat anti-rabbit IgG (H + L), or Anti-rabbit IgG (whole molecule)-fluorescein isothiocyanate (FITC) antibody produced in goat and Invitrogen™ Do anti-Ms IgG Secondary Antibody TRITC conjugate RT. Thereafter, the nucleus was counterstained with 4,6-diamino-2-phenylindole (DAPI) for 5 min, mounted with anti-fluorescence quenching agent, and observed with a fluorescence microscope (Olympus, Tokyo, Japan).

2.12. Western Blot analysis

Cells and lung tissue samples were equally lysed in radioimmunoprecipitation assay (RIPA) with protease and phosphatase inhibitors for 30 min, followed by centrifugation at 12,000 rpm for 15 min at 4 °C. The supernatant was then transferred to new centrifugal tubes and stored at −20 °C. Concentrations of proteins were assayed using a BCA protein assay kit. Equal amounts of protein were separated by 10% sodium dodecyl sulfate-polyacrylamide gel electrophoresis (SDS-PAGE) and electrophoretically transferred to polyvinylidene difluoride membranes (PVDFs). The membranes were blocked with 5% (w/v) nonfat dry milk for 2 h and incubated overnight with specific primary antibody at 4 °C. Thereafter, the membranes were interacted with HRP-conjugated secondary antibody for an additional 2 h at room temperature after being thoroughly washed three times with tri-buffered saline tween (TBST). Bands were detected by electrochemiluminescence (ECL) and quantified using Carestream MI SE analysis software.

2.13. Statistical analysis

All data in the different experimental groups are expressed as mean ± standard error of the mean (SEM). Differences between the groups were assessed by a one-way ANOVA and the Bonferroni multiple comparisons test, which were analyzed using GraphPad PRISM

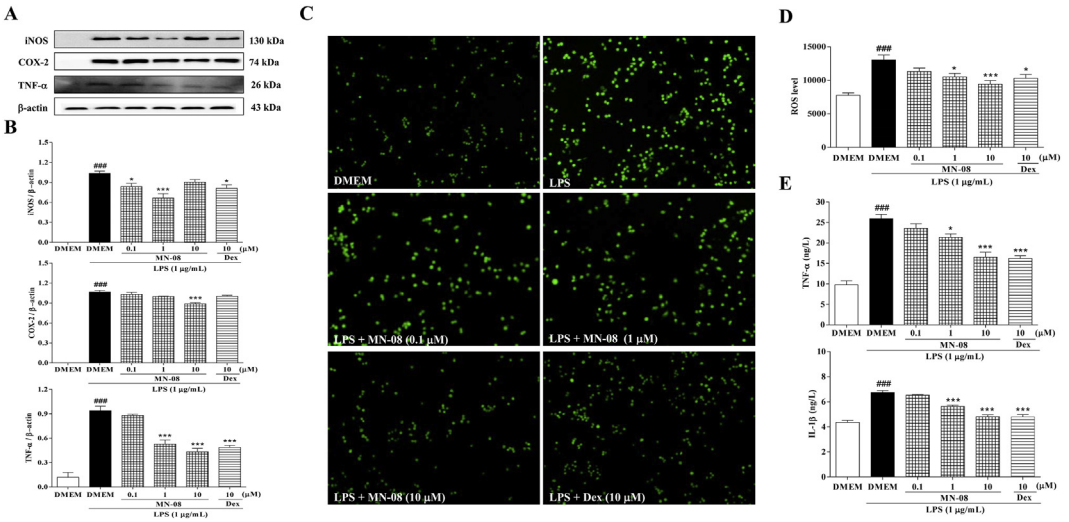

Fig. 2. MN-08 restrains inflammatory response and oxidative damage in LPS-induced RAW 264.7 cells. (A–B) iNOS, COX-2, TNF-α protein expressions were normalized to that of β-actin by Western Blot analysis. (C–D) ROS generation was measured by DCFH-DA fluorescence probe. (E) The effect of MN-08 on LPS-induced TNF-α and IL-1β production in RAW 264.7 cells by ELISA assay. All data were expressed as means ± SEM based on 3 independent experiments. $^{###}p < 0.001$ (relative to DMEM). $^{***}p < 0.001$, $^{*}p < 0.05$ (relative to LPS).

software (GraphPad Software Inc., Avenida, CA, USA). Significant differences were represented as $p < 0.05$.

3. Results

3.1. Cytotoxicity of MN-08 in RAW 264.7 cells and A549 cells

An MTT assay was used to investigate the effects of MN-08 in RAW 264.7 and A549 cells. As shown in Fig. 1B, MN-08 (0.01–10 μM) had no obvious toxicity on RAW 264.7 and A549 cells after 24 h of treatment. As a result, the concentrations of MN-08 (0.1, 1, and 10 μM) were applied in the subsequent experiment.

3.2. MN-08 restrains inflammatory response and oxidative damage in LPS-induced RAW 264.7 cells

The protein expression of TNF-α, iNOS, and COX-2 were markedly increased in LPS-induced RAW 264.7 cells, whereas MN-08 treatment considerably inhibited production of the inflammatory mediators by immunoblotting (Fig. 2A–B). In addition, MN-08 and Dex effectively decreased the level of ROS formation in LPS-induced RAW 264.7 cells' oxidative damage by fluorescence microplate reader (Fig. 2C–D). Moreover, we observed that RAW 264.7 cells exposed to LPS upregulated protein expression of TNF-α and IL-1β in comparison to the DMEM group. The elevation was dramatically decreased after MN-08 treatment in a concentration-dependent manner (Fig. 2E).

3.3. MN-08 inhibits LPS-induced the activation of inflammatory signaling and improves peroxiredoxins expression in RAW 264.7 cells

The MAPKs signaling pathways play a crucial part in cellular inflammation, which modifies a vast number of pro-inflammatory cytokines. We designed this experiment to investigate three key kinases of p38 MAPK, JNK, and ERK-participation in phosphorylation levels. As shown in Fig. 3A–B, LPS treatment resulted in the elevation of phosphorylation levels of p38 MAPK, JNK, and ERK, which signified the activation of the MAPKs pathways. Nevertheless, treatment with MN-08 protected the RAW 264.7 cells from the MAPKs phosphorylations. These results validated that MN-08 affected the MAPKs pathways by acting upstream of the target proteins.

Furthermore, the phosphorylations of MAPKs are well-known to induce NF-κB activation and increase iNOS gene expression [36]. To explore the molecular mechanisms of MN-08 in LPS-induced RAW 264.7 cells, we evaluated the protein expression of p-IκBα and p-NF-κB p65 by immunoblotting. As illustrated in Fig. 3C–D, LPS obviously stimulated the expression of p-IκBα and p-NF-κB p65, and treatment with MN-08 significantly attenuated the LPS-induced phosphorylation of NF-κB p65. These results indicated that MN-08 might inhibit LPS-induced IκBα degradation and NF-κB p65 nuclear translocation in RAW 264.7 cells.

HO-1 expression plays a crucial role in cytoprotective response in diverse pathological conditions because of its anti-inflammatory and anti-oxidative properties [37]. We theorized that MN-08 could mediate the induction of HO-1 in LPS-induced RAW 264.7 cells, which was determined by Western Blot analysis. Our data showed that treatment with MN-08 could increase HO-1 protein expression in RAW 264.7 cells with LPS-induced oxidative damage (Fig. 3E–F).

3.4. MN-08 upregulates Bcl-2/Bax ratio and tight junction structure protein expression in LPS-induced A549 cells

The expression of Bcl-2 and Bax proteins were evaluated to find the mechanism of MN-08 protection in apoptosis of A549 cells after exposure to LPS. In contrast with elevated Bax protein level, the protein level of Bcl-2 was apparently lowered by LPS administration. However, MN-08 enhanced the expression of Bcl-2 and decreased that of Bax (Fig. 4A–B). Accumulating reports indicate that expression of tight junction protein family members are known to be critical for maintenance of barrier function in pulmonary epithelial cells [38,39]. Therefore, we further verified the effect of MN-08 on the TJs structure of cells in the LPS-induced A549 cells apoptosis model. The results showed that MN-08 (10 μM) significantly improved ZO-1, occludin, JAM-1, and Claudin-1 protein expressions in LPS-induced A549 cells (Fig. 4C–F).

3.5. MN-08 eliminates lung edema and permeability changes

The lung W/D ratio measures the severity of lung edema. As shown in Fig. 5A, administration of LPS alone increased the level of lung W/D ratio, which was significantly reduced by MN-08, Dex, and Mem treatments. Moreover, the damage of pulmonary capillary integrity, which is a vital characteristic of LPS-induced ALI, causes an increase in

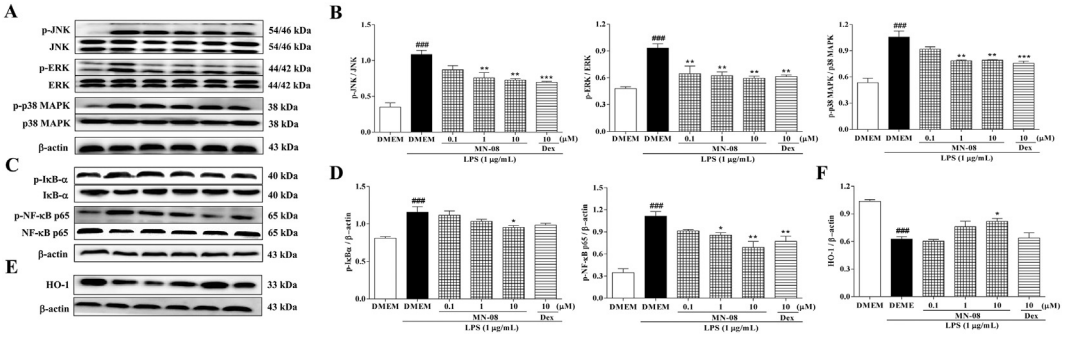

Fig. 3. MN-08 inhibits LPS-induced the activation of inflammatory signaling and improves peroxiredoxins expression in RAW 264.7 cells. (A–B) Quantification of relative expression of p-JNK/JNK, p-ERK/ERK, and p-p38 MAPK/p38 MAPK. (C–D) Quantification of p-IκBα and p-NF-κB p65 expressions were normalized to that of β-actin. (E–F) Quantification of HO-1 expression were normalized as β-actin. All data were expressed as means ± SEM based on 3 independent experiments. $^{###}p < 0.001$ (relative to DMEM). $^{***}p < 0.001$, $^{**}p < 0.01$, $^{*}p < 0.05$ (relative to LPS).

permeability and is typically caused by increased protein levels in BALF. As shown in Fig. 5B, compared to the mice in the NS group, LPS treatment moderately increased the total protein concentration in BALF. Although drug treatments slightly reduced total protein content, there were no significant differences between drug groups and the LPS group in lung permeability.

3.6. MN-08 represses inflammatory response and oxidative damage in lung tissue

We assumed that the LPS challenge could release glutamate abnormally in lungs to validate whether or not overproduction of glutamate could cause an inflammatory response and oxidative damage. The results in Fig. 6A indicate that glutamate content in lungs was higher in the LPS group than that in the NS group, but it was dramatically decreased by MN-08 (12.5 mg/kg).

In addition, to further investigate the anti-inflammation activities of MN-08, cells counts in BALF were determined in this study. As depicted in Fig. 6B, total cell, neutrophil, and macrophage counts were obviously increased in the LPS group. However, MN-08 intervention largely reduced the number of total cells, neutrophils, and macrophages in a dose-dependent manner. Besides, IHC for Gr-1 demonstrated that the modestly-injured lungs in mice in the drugs group contained significantly fewer infiltrating neutrophil compared with the LPS group. Mac-2-staining also revealed significantly fewer macrophages per areas of lungs in the drugs group than in the LPS group (Fig. 7B). Furthermore, MPO activity was used to assess neutrophil accumulation in the lung tissue. As illustrated in Fig. 6C, MPO activity was significantly increased in the LPS group; however, MN-08, Dex, and Mem markedly inhibited MPO activity.

Inflammatory cytokines and mediators play important roles in the physiopathology of LPS-induced ALI. Thus, we measured TNF-α and IL-

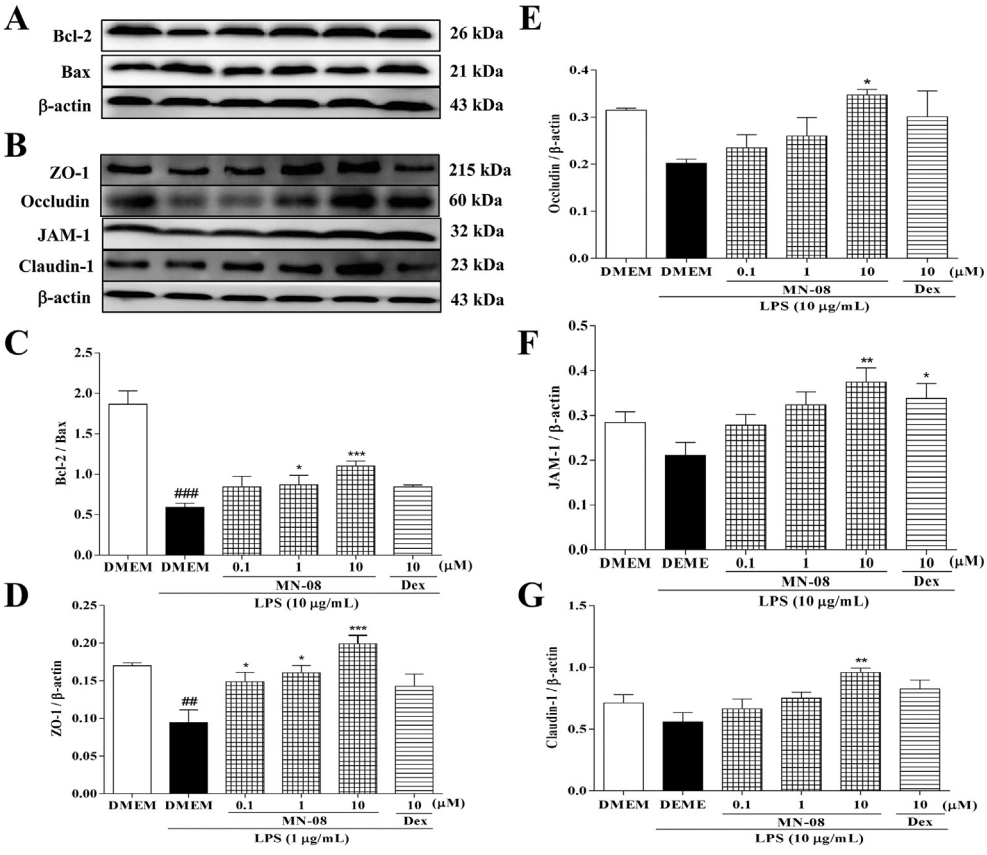

Fig. 4. MN-08 up-regulates Bcl-2/Bax ratio and tight junction structure protein expressions in LPS-induced A549 cells. (A–B) Quantification of Bax and Bcl-2 expression were normalized to that of β-actin. (C–F) Quantification of ZO-1, occludin, JAM-1 and Claudin-1 expressions were normalized as β-actin. All data were expressed as means ± SEM based on 3 independent experiments. $^{###}p < 0.001$, $^{##}p < 0.01$ (relative to DMEM). $^{***}p < 0.001$, $^{**}p < 0.01$, $^{*}p < 0.05$ (relative to LPS).

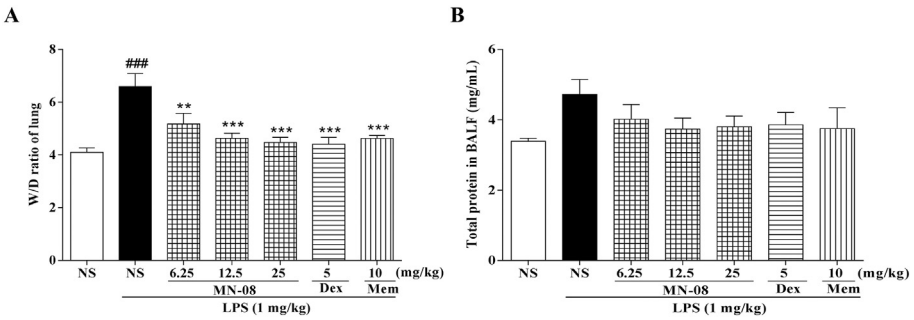

Fig. 5. MN-08 eliminates lung edema and permeability changes. (A) The ratio of wet lung to dry lung was calculated to assess tissue edema. (B) BALF was collected after LPS challenge to measure the total protein by BCA kits. All data were expressed as means ± SEM based on 8 mice in per group. $^{###}p < 0.001$ (relative to NS). $^{***}p < 0.001$, $^{**}p < 0.01$(relative to LPS).

1β levels for inflammatory response. Furthermore, we examined SOD, MDA, GSH, and HO-1 activity for oxidative damage. We found that levels of TNF-α and IL-1β and MDA in lungs were reduced dramatically (Fig. 6D, E, H, I), whereas the levels of SOD, GSH, and HO-1 were obviously elevated by MN-08 (Fig. 6F–G, J).

3.7. MN-08 ameliorates pulmonary histopathological changes

Histological analysis was used to evaluate the protective effects of MN-08 in LPS-induced ALI. Pathological changes were observed in the LPS group, which include interstitial edema, hemorrhage, thickening of the alveolar wall, and inflammatory cells infiltration (Fig. 7A, D). However, to varying degrees, MN-08 and Dex ameliorated lung injury. In addition, immunohistochemical staining demonstrated that LPS reduced tight junction protein expressions including ZO-1 and JAM-1 in response to LPS challenge. Treatment with MN-08, Dex, and Mem increased their expressions (Fig. 7C, E, F).

3.8. MN-08 suppresses the activation of inflammatory signaling pathway in lung tissue

To investigate whether the suppression of inflammatory response by MN-08 in LPS-induced ALI was mediated via the MAPKs pathways, we evaluated the effects of MN-08 in LPS-induced activation of the phosphorylation of p38 MAPK, ERK, and JNK levels. As shown in Fig. 8A–B, the phosphorylation of p38 MAPK, ERK, and JNK were increased in LPS-induced ALI. However, MN-08 significantly downregulated the phosphorylation levels of MAPKs signaling in the ALI model. Studies have shown that MAPKs phosphorylations typically induce NF-κB activation and increases pro-inflammatory cytokine secretion [40,41]. Therefore, we investigated whether MN-08 inhibited the phosphorylation of IκBα and NF-κB p65 in lungs. As demonstrated in Fig. 8C–D, the phosphorylation levels of IκBα and NF-κB p65 were increased in LPS-induced ALI. Nevertheless, MN-08 treatment markedly inhibited the NF-κB p65 phosphorylation. These results suggest that MN-08 might exert its lung protection on LPS-induced ALI by inhibiting the MAPKs/NF-κB pathways.

4. Discussion

ALI is emblematic of an intense pulmonary inflammatory response, involving neutrophil recruitment, interstitial edema, a disruption of epithelial integrity, and lung parenchymal injury. The pathogenesis of ALI involves disorders of inflammatory/anti-inflammatory balance and oxidant/anti-oxidant balance, including the increased production of pro-inflammatory cytokines, the abnormal secretion of chemokines, and the formation of ROS [42]. Mouse models of ALI administered by intratracheal instillation of LPS have been very useful in providing some direction into the mechanisms related to disease pathogenesis, and creating opportunities to explore novel and innovative therapeutic targets. Although many studies that focused on the pathophysiology of ALI have been performed, the effective therapies have not been available. However, it is noteworthy that we designed and synthesized a novel Memantine derivative MN-08 that acts in the role of NMDAR antagonism in our previous research. This study was to evaluate whether MN-08 exerts anti-inflammatory and anti-oxidative effects in LPS-induced cells and animal models of ALI.

NMDARs are ionotropic glutamate receptors. In the CNS, overstimulation of NMDAR leads to excitotoxic neuronal cell death under many conditions, including ischemic stroke, traumatic brain injury, Alzheimer disease, Parkinson disease, and epilepsy. In addition, NMDAR activation induces neuroinflammation. It is worth emphasizing that glutamate is released by astrocytes and activates microglia during neuroinflammation. NMDAR expression has been demonstrated, and glutamate has been shown to induce excitotoxic changes that are inhibited by receptor antagonists [43,44]. However, the mechanisms of ALI induced by activation of NMDAR are not completely understood. In our previous study, glutamate was increased by LPS-induced mice lung injury and was decreased by MN-08 treatment. Our results indicated that MN-08 might suppress glutamate influx via inhibiting NMDAR.

Inflammation and oxidative stress are acknowledged as interrelated biological events that both are related to the pathogenesis of ALI. LPS administration could trigger excessive release of cytokines, chemokines, and ROS [45,46]. Moreover, previous reports have suggested that neutrophils and macrophages play an essential role in the regulation of inflammation responses [47,48]. In our preliminary study, MN-08 treatment considerably inhibited the production of the cytokines TNF-α, IL-1β, iNOS, and COX-2 and effectively decreased the level of ROS formation in RAW 264.7 cells. More importantly, we found that MN-08 could suppressed TNF-α and IL-1β and secretion in LPS-induced mice blood plasma. Based on these outcomes, we further investigated whether the role played by MN-08 in mice with LPS-induced ALI was protective. We examined SOD, MDA, and GSH content for further exploration. SOD acts as a natural scavenger for biological oxygen-free radicals and has wide medical value, including the treatment of rheumatoid arthritis, chronic polyarthritis, myocardial infarction, cardiovascular disease, tumor, and radiation therapy in patients with inflammatory disease. GSH exerts the main anti-oxidation and anti-aging physiological function through scavenging free radicals. Our results showed that MN-08 (25 mg/kg) could increase SOD activity and GSH content in LPS-induced ALI. However, MDA is one of the most important products of membrane lipid peroxidation, and it can damage the cell membrane, promote the body's aging, and induce tumor or atherosclerosis. Our data showed that treatment with MN-08 (25 mg/kg) decreased MDA content compared with the LPS group. Therefore, any approach that inhibits oxidative stress and inflammation in vitro and in vivo may potentially have an effect on the prevention or treatment of ALI.

Inflammatory response and oxidative damage could cause pulmonary epithelial cell apoptosis and destroy cell TJs, causing pulmonary edema and permeability changes. To quantify the changes of pulmonary edema, we evaluated the W/D ratio of the lung. Our results showed that MN-08 significantly inhibited lung edema. TJs are multiprotein complexes located at sites of cell-cell contact and are composed

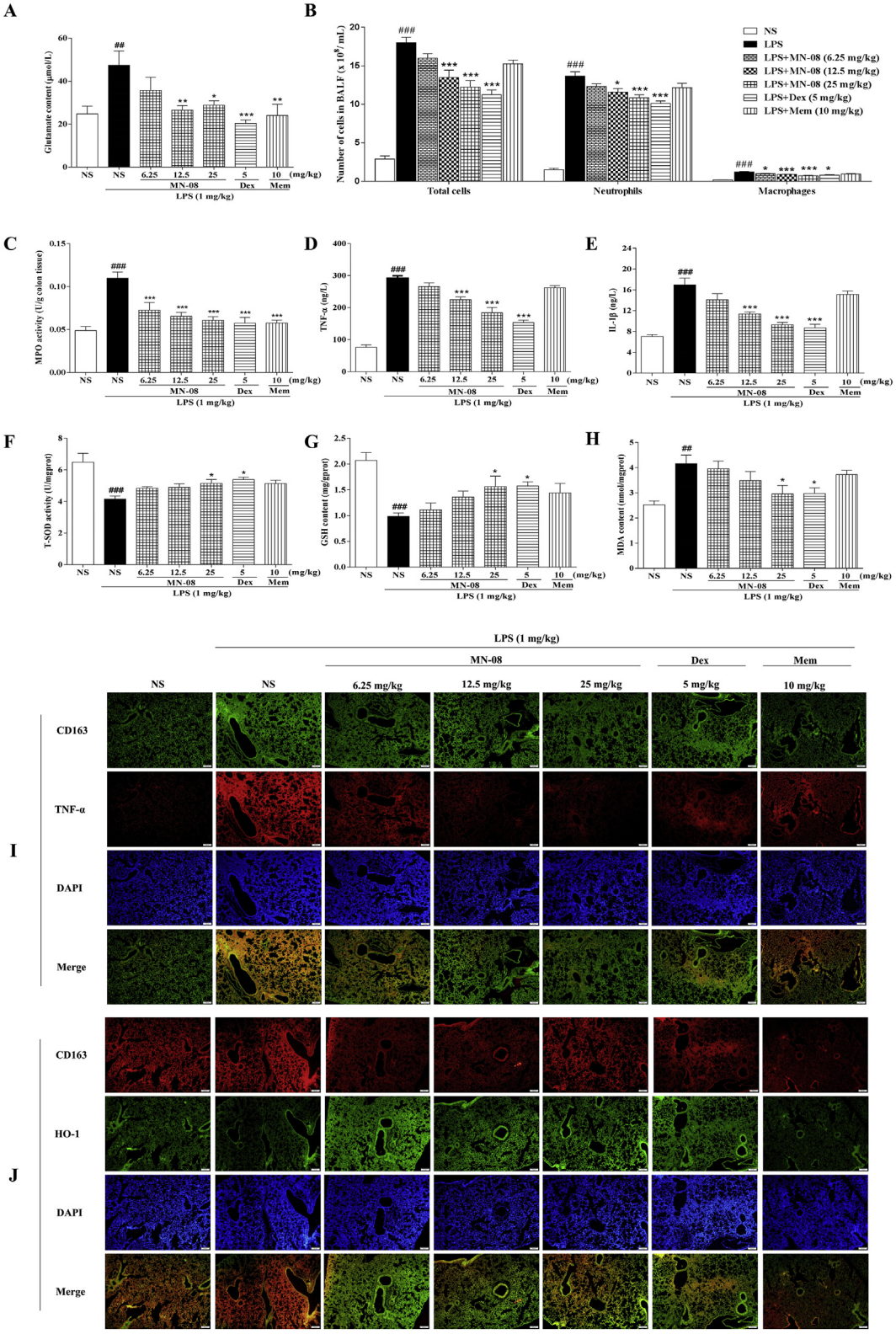

Fig. 6. MN-08 reduces inflammatory response and oxidative damage in lung tissues. Lungs were obtained to measure the Glutamate content (A), MPO activity (C), T-SOD activity (F), GSH content (G) and MDA content (H) by using commercially available assay kits. BALF was collected to total cells, neutrophils and macrophages counts (B). Plasma was harvested for measure the TNF-α (D) and IL-1β (E) by ELISA kits assay. The lung sections were stained with anti-CD163 (I, J), anti-TNF-α (I) and anti-HO-1 (J) by immunofluorescence (magnification × 400). All data were expressed as means ± SEM based on 8 mice in per group. $^{###}p < 0.001$, $^{##}p < 0.01$ (relative to NS). $^{***}p < 0.001$, $^{**}p < 0.01$, $^{*}p < 0.05$ (relative to LPS).

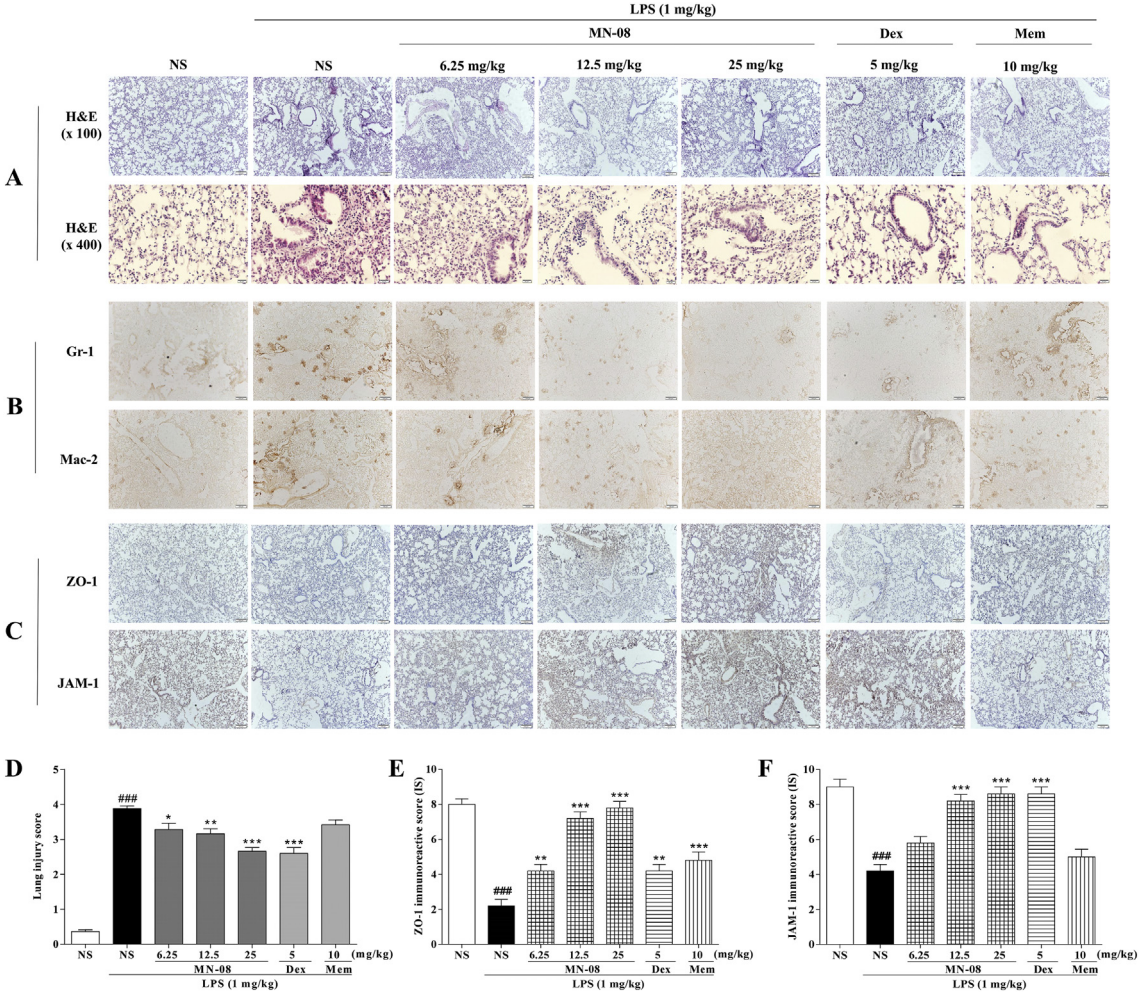

Fig. 7. MN-08 ameliorates pulmonary histopathological changes. Lungs were collected to evaluate pathological of lung injury. (A) Representative histological sections of the lungs were stained with H&E (magnification × 100 and ×400). (B) Immunohistochemistry of neutrophils and macrophages in lung tissues evaluation, the following antibodies were used: mouse anti-rabbit Gr-1 antibody, mouse anti-rabbit Mac-2 antibody (magnification × 100). (C) The lung sections were stained with anti-Zonula occludens 1 (ZO-1) and anti-Junctional Adhesion Molecule 1 (JAM-1) by immunohistochemistry (magnification × 100). (D) The lung injury score was determined following a five-point scale from 0 to 4 as follows: no damage = 0, mild damage = 1, moderate damage = 2, severe damage = 3, and very severe damage = 4, respectively. (E–F) The immunoreactive score (IS) was determined based on the percentage of positive signal (brown color) and the staining intensity: weak staining = 1, moderate = 2, and strong = 3, respectively. All data were expressed as means ± SEM based on random 5 mice in per group. $^{###}p < 0.001$ (relative to NS). $^{***}p < 0.001$, $^{**}p < 0.01$, $^{*}p < 0.05$ (relative to LPS). (For interpretation of the references to color in this figure legend, the reader is referred to the web version of this article.)

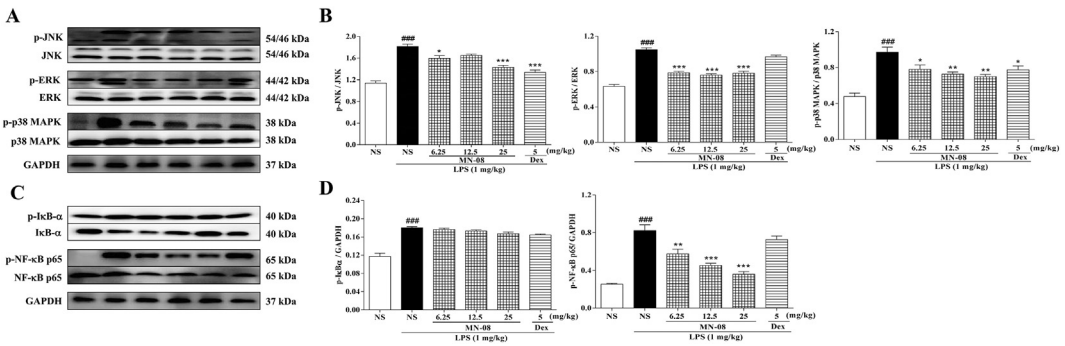

Fig. 8. MN-08 suppresses activation of inflammatory signaling in lung tissue. (A–B) Quantification of relative expression of p-JNK/JNK, p-ERK/ERK, and p-p38 MAPK/p38 MAPK. (C-D) Quantification of p-IκBα and p-NF-κB p65 expressions were normalized to that of GADPH. All data were expressed as means ± SEM based on random 3 mice in per group. $^{###}p < 0.001$ (relative to NS). $^{***}p < 0.001$, $^{**}p < 0.01$, $^{*}p < 0.05$ (relative to LPS).

of transmembrane, cytosolic, and cytoskeletal proteins that together produce a selective barrier to water, ions, and soluble molecules [49]. MN-08 treatment significantly improved ZO-1, occludin, JAM-1, and Claudin-1 protein expressions in LPS-induced A549 cells. Immunohistochemical staining showed that MN-08 significantly improved TJs expression compared with the LPS group. H&E staining showed that it is common and conspicuous for the infiltration of pro-inflammatory cells, hemorrhage, alveolar edema, and airway epithelial necrosis in the LPS group but rarely obvious in the MN-08, Dex, and Mem treatment groups. There exists the increased MPO activity with the infiltration of neutrophils in the lung during ALI. Therefore, MPO activity, a marker of neutrophil influx into tissue and directly proportional to the number of neutrophils in the tissue, was studied. Our present data illustrated increased MPO activity in the lung tissue in an LPS-induced ALI model, which was consistent with the histopathological changes of leukocyte infiltration, whereas such increase was significantly reduced by MN-08. We demonstrated that MN-08 dramatically suppressed lung injury in mice.

To further explore the possible underlying mechanism of ALI induced by LPS, the effects of MN-08 on MAPKs/NF-κB pathways were examined. NF-κB is a central and critical factor regulating the production of inflammatory mediators. NF-κB consists of p65, p50, and IκBα subunits [50]. The activation of NF-κB is vital to the pathogenesis of many inflammatory lung disorders, including chronic obstructive pulmonary disease, asthma, pneumonia, and ALI. Increasing studies demonstrate that MAPKs signaling pathways regulated the activation of NF-κB. MAPKs, including ERK, JNK, and p38 MAPK, play critical roles in the regulation of inflammatory responses [9,10,40]. Here, we found that MAPKs and NF-κB were spontaneously activated during an LPS attack, and pre-treatment of MN-08 inhibited the phosphorylation of MAPKs and NF-κB in a dose-dependent manner both in vivo and in vitro. Furthermore, Nrf2 is a major factor prompting the expression of various antioxidant genes in response to a great number of harmful stimulants including against inflammation and oxidative stress. HO-1 is the major anti-inflammatory and anti-oxidative enzyme that is mediated by Nrf2 activation [12,13,30]. Our results confirmed that MN-08 could alleviate the severity of lung injury, as suggested by the significant upregulations of HO-1 expressions in LPS-induced RAW 264.7 cells.

5. Conclusion

In summary, our study indicates that MN-08 exerts lung protection in LPS-induced acute lung injury both in vitro and in vivo via anti-inflammatory and anti-oxidative activities. MN-08 might hold promise as a novel drug to treat ALI due to its underlying NMDAR target.

Competing interests

The authors declare that they have no conflicting interests.

Acknowledgments

This work was supported by grants from the National Natural Science Foundation of China (81673496) and the Science and Technology Planning Project of Guangdong Province, China (2015B020211011).

References

[1] J.V. Diaz, R. Brower, C.S. Calfee, M.A. Matthay, Therapeutic strategies for severe acute lung injury, Crit. Care Med. 38 (8) (2010) 1644–1650.
[2] G.R. Bernard, A. Artigas, K.L. Brigham, J. Carlet, K. Falke, L. Hudson, M. Lamy, J.R. LeGall, A. Morris, R. Spragg, Report of the American-European Consensus conference on acute respiratory distress syndrome: definitions, mechanisms, relevant outcomes, and clinical trial coordination. Consensus Committee, J. Crit. Care 9 (1) (1994) 72–81.
[3] T.J. Standiford, P.A. Ward, Therapeutic targeting of acute lung injury and acute respiratory distress syndrome, Transl. Res. 167 (1) (2016) 183–191.
[4] K.L. Brigham, R. Bowers, J. Haynes, Increased sheep lung vascular permeability caused by *Escherichia coli* endotoxin, Circ. Res. 45 (2) (1979) 292–297.
[5] F. Aeffner, B. Bolon, I.C. Davis, Mouse models of acute respiratory distress syndrome: a review of analytical approaches, pathologic features, and common measurements, Toxicol. Pathol. 43 (8) (2015) 1074–1092.
[6] T. Yokochi, A new experimental murine model for lipopolysaccharide-mediated lethal shock with lung injury, Innate Immun. 18 (2) (2012) 364–370.
[7] M.A. Taddonio, V. Dolgachev, M. Bosmann, P.A. Ward, G. Su, S.C. Wang, M.R. Hemmila, Influence of lipopolysaccharide-binding protein on pulmonary inflammation in gram-negative pneumonia, Shock 43 (6) (2015) 612–619.
[8] M.W. Covert, T.H. Leung, J.E. Gaston, D. Baltimore, Achieving stability of lipopolysaccharide-induced NF-kappaB activation, Science 309 (5742) (2005) 1854–1857.
[9] R. Feng, Y. Lu, L.L. Bowman, Y. Qian, V. Castranova, M. Ding, Inhibition of activator protein-1, NF-kappaB, and MAPKs and induction of phase 2 detoxifying enzyme activity by chlorogenic acid, J. Biol. Chem. 280 (30) (2005) 27888–27895.
[10] R.B. Goodman, J. Pugin, J.S. Lee, M.A. Matthay, Cytokine-mediated inflammation in acute lung injury, Cytokine Growth Factor Rev. 14 (6) (2003) 523–535.
[11] J.E. Repine, N.D. Elkins, Effect of ergothioneine on acute lung injury and inflammation in cytokine insufflated rats, Prev. Med. 54 (2012) S79–S82 (Suppl.).
[12] T. Nguyen, P.J. Sherratt, H.C. Huang, C.S. Yang, C.B. Pickett, Increased protein stability as a mechanism that enhances Nrf2-mediated transcriptional activation of the antioxidant response element. Degradation of Nrf2 by the 26 S proteasome, J. Biol. Chem. 278 (7) (2003) 4536–4541.
[13] T.W. Kensler, N. Wakabayashi, S. Biswal, Cell survival responses to environmental stresses via the Keap1-Nrf2-ARE pathway, Annu. Rev. Pharmacol. Toxicol. 47 (2007) 89–116.
[14] C.E. Overgaard, B.L. Daugherty, L.A. Mitchell, M. Koval, Claudins: control of barrier function and regulation in response to oxidant stress, Antioxid. Redox Signal. 15 (5) (2011) 1179–1193.
[15] O.H. Wittekindt, Tight junctions in pulmonary epithelia during lung inflammation, Pflugers Arch. 469 (1) (2017) 135–147.
[16] V.E. Ryman, N. Packiriswamy, L.M. Sordillo, Role of endothelial cells in bovine mammary gland health and disease, Anim. Health Res. Rev. 16 (2) (2015) 135–149.
[17] S. Herold, N.M. Gabrielli, I. Vadasz, Novel concepts of acute lung injury and alveolar-capillary barrier dysfunction, Am. J. Phys. Lung Cell. Mol. Phys. 305 (10) (2013) L665–L681.
[18] B. Schlingmann, C.E. Overgaard, S.A. Molina, K.S. Lynn, L.A. Mitchell, S. Dorsainvil White, A.L. Mattheyses, D.M. Guidot, C.T. Capaldo, M. Koval, Regulation of claudin/zonula occludens-1 complexes by hetero-claudin interactions, Nat. Commun. 7 (2016) 12276.
[19] D. Gunzel, A.S. Yu, Claudins and the modulation of tight junction permeability, Physiol. Rev. 93 (2) (2013) 525–569.
[20] J.T. Coyle, S.J. Bird, R.H. Evans, R.L. Gulley, J.V. Nadler, W.J. Nicklas, J.W. Olney, Excitatory amino acid neurotoxins: selectivity, specificity, and mechanisms of action. Based on an NRP one-day conference held June 30, 1980, Neurosci. Res. Program Bull. 19 (4) (1981) 1–427.
[21] N. Inagaki, H. Kuromi, T. Gonoi, Y. Okamoto, H. Ishida, Y. Seino, T. Kaneko, T. Iwanaga, S. Seino, Expression and role of ionotropic glutamate receptors in pancreatic islet cells, FASEB J. 9 (8) (1995) 686–691.
[22] N.F. Gonzalez-Cadavid, I. Ryndin, D. Vernet, T.R. Magee, J. Rajfer, Presence of NMDA receptor subunits in the male lower urogenital tract, J. Androl. 21 (4) (2000) 566–578.
[23] A. Deng, J.M. Valdivielso, K.A. Munger, R.C. Blantz, S.C. Thomson, Vasodilatory *N*-methyl-D-aspartate receptors are constitutively expressed in rat kidney, J. Am. Soc. Nephrol. 13 (5) (2002) 1381–1384.
[24] K.G. Dickman, J.G. Youssef, S.M. Mathew, S.I. Said, Ionotropic glutamate receptors in lungs and airways: molecular basis for glutamate toxicity, Am. J. Respir. Cell Mol. Biol. 30 (2) (2004) 139–144.
[25] G. Lombardi, C. Dianzani, G. Miglio, P.L. Canonico, R. Fantozzi, Characterization of ionotropic glutamate receptors in human lymphocytes, Br. J. Pharmacol. 133 (6) (2001) 936–944.
[26] Y. Wang, W. Liu, X. Liu, M. Sheng, Y. Pei, R. Lei, S. Zhang, R. Tao, Role of liver in modulating the release of inflammatory cytokines involved in lung and multiple organ dysfunction in severe acute pancreatitis, Cell Biochem. Biophys. 71 (2) (2015) 765–776.
[27] C. Luo, F. Luo, Y. Sun, L. Xu, P. Yu, Y. Wang, Z. Zhang, Pharmacokinetics of memantine-derivative MN-08 in rats: a preclinical study, J. Pharm. Biomed. Sci. 7 (10) (2017).
[28] Z. Liu, S. Yang, X. Jin, et al., Synthesis and biological evaluation of memantine nitrates as a potential treatment for neurodegenerative diseases, Med. Chem. Commun. 8 (2017) 135–147.
[29] Q. Jiang, M. Yi, Q. Guo, C. Wang, H. Wang, S. Meng, C. Liu, Y. Fu, H. Ji, T. Chen, Protective effects of polydatin on lipopolysaccharide-induced acute lung injury through TLR4-MyD88-NF-kappaB pathway, Int. Immunopharmacol. 29 (2) (2015) 370–376.
[30] J. Wang, Y. Nie, Y. Li, Y. Hou, W. Zhao, J. Deng, P.G. Wang, G. Bai, Identification of target proteins of mangiferin in mice with acute lung injury using functionalized magnetic microspheres based on click chemistry, J. Agric. Food Chem. 63 (45) (2015) 10013–10021.
[31] H. Lv, Z. Yu, Y. Zheng, L. Wang, X. Qin, G. Cheng, X. Ci, Isovitexin exerts anti-inflammatory and anti-oxidant activities on lipopolysaccharide-induced acute lung injury by inhibiting MAPK and NF-kappaB and activating HO-1/Nrf2 pathways, Int. J. Biol. Sci. 12 (1) (2016) 72–86.

[32] C. Li, D. Yang, X. Cao, F. Wang, H. Jiang, H. Guo, L. Du, Q. Guo, X. Yin, LFG-500, a newly synthesized flavonoid, attenuates lipopolysaccharide-induced acute lung injury and inflammation in mice, Biochem. Pharmacol. 113 (2016) 57–69.
[33] C. Lei, Y. Jiao, B. He, G. Wang, Q. Wang, J. Wang, RIP140 down-regulation alleviates acute lung injury via the inhibition of LPS-induced PPARgamma promoter methylation, Pulm. Pharmacol. Ther. 37 (2016) 57–64.
[34] G. Ayaz, Z. Halici, A. Albayrak, E. Karakus, E. Cadirci, Evaluation of 5-HT7 receptor trafficking on in vivo and in vitro model of lipopolysaccharide (LPS)-induced inflammatory cell injury in rats and LPS-treated A549 cells, Biochem. Genet. 55 (1) (2017) 34–47.
[35] L. Shao, D. Meng, F. Yang, H. Song, D. Tang, Irisin-mediated protective effect on LPS-induced acute lung injury via suppressing inflammation and apoptosis of alveolar epithelial cells, Biochem. Biophys. Res. Commun. 487 (2) (2017) 194–200.
[36] C. Chen, Y.H. Chen, W.W. Lin, Involvement of p38 mitogen-activated protein kinase in lipopolysaccharide-induced iNOS and COX-2 expression in J774 macrophages, Immunology 97 (1) (1999) 124–129.
[37] T.S. Lee, H.L. Tsai, L.Y. Chau, Induction of heme oxygenase-1 expression in murine macrophages is essential for the anti-inflammatory effect of low dose 15-deoxy-Delta 12,14-prostaglandin J2, J. Biol. Chem. 278 (21) (2003) 19325–19330.
[38] C.E. Overgaard, L.A. Mitchell, M. Koval, Roles for claudins in alveolar epithelial barrier function, Ann. N. Y. Acad. Sci. 1257 (2012) 167–174.
[39] B. Schlingmann, S.A. Molina, M. Koval, Claudins: gatekeepers of lung epithelial function, Semin. Cell Dev. Biol. 42 (2015) 47–57.
[40] M.S. Hayden, S. Ghosh, Shared principles in NF-kappaB signaling, Cell 132 (3) (2008) 344–362.
[41] M. Gadina, N. Gazaniga, L. Vian, Y. Furumoto, Small molecules to the rescue: inhibition of cytokine signaling in immune-mediated diseases, J. Autoimmun. 85 (2017) 20–31.
[42] P. Stormann, T. Lustenberger, B. Relja, I. Marzi, S. Wutzler, Role of biomarkers in acute traumatic lung injury, Injury 48 (11) (2017) 2400–2406.
[43] S.I. Said, H. Pakbaz, H.I. Berisha, S. Raza, NMDA receptor activation: critical role in oxidant tissue injury, Free Radic. Biol. Med. 28 (8) (2000) 1300–1302.
[44] E.K. Hamasato, A.P. Ligeiro de Oliveira, A. Lino-dos-Santos-Franco, A. Ribeiro, V. Ferraz de Paula, J.P. Peron, A.S. Damazo, W. Tavares-de-Lima, J. Palermo-Neto, Effects of MK-801 and amphetamine treatments on allergic lung inflammatory response in mice, Int. Immunopharmacol. 16 (4) (2013) 436–443.
[45] M. Bhatia, S. Moochhala, Role of inflammatory mediators in the pathophysiology of acute respiratory distress syndrome, J. Pathol. 202 (2) (2004) 145–156.
[46] J.W. Semple, M. Kim, J. Hou, M. McVey, Y.J. Lee, A. Tabuchi, W.M. Kuebler, Z.W. Chai, A.H. Lazarus, Intravenous immunoglobulin prevents murine antibody-mediated acute lung injury at the level of neutrophil reactive oxygen species (ROS) production, PLoS One 7 (2) (2012) e31357.
[47] Y. Zhang, L. Guan, J. Yu, Z. Zhao, L. Mao, S. Li, J. Zhao, Pulmonary endothelial activation caused by extracellular histones contributes to neutrophil activation in acute respiratory distress syndrome, Respir. Res. 17 (1) (2016) 155.
[48] C.H. Han, P.X. Zhang, W.W. Liu, Macrophage polarization is related to the pathogenesis of decompression induced lung injury, Med. Gas Res. 7 (3) (2017) 220–223.
[49] L.A. Mitchell, C. Ward, M. Kwon, P.O. Mitchell, D.A. Quintero, A. Nusrat, C.A. Parkos, M. Koval, Junctional adhesion molecule A promotes epithelial tight junction assembly to augment lung barrier function, Am. J. Pathol. 185 (2) (2015) 372–386.
[50] Y.J. Surh, K.S. Chun, H.H. Cha, S.S. Han, Y.S. Keum, K.K. Park, S.S. Lee, Molecular mechanisms underlying chemopreventive activities of anti-inflammatory phytochemicals: down-regulation of COX-2 and iNOS through suppression of NF-kappa B activation, Mutat. Res. 480–481 (2001) 243–268.